NUMERICAL ANALYSIS OF OPTIMAL FOURTH-HARMONIC-GENERATION CRYSTAL LENGTH FOR WAVELENGTH CONVERSION INTO ULTRAVIOLET LIGHT

Takafumi Ohfuchi[1,*], Toshio Takiya[1], Norihiro Inoue[1], Koh-ichirow Nakayama[1], Naoaki Fukuda[2] & Hiroshi Kumagai[3]

[1]Technical Research Institute, Hitachi Zosen Corporation, 2-2-11 Funa-machi, Taisho-ku, Osaka 551-0022, Japan
[2]Office of Society-Academia Collaboration for Innovation, Kyoto University, 1-39-2204 Goryo-Ohara, Nishikyo-ku, Kyoto 615-8245, Japan
[3]School of Allied Health Sciences, Kitasato University, 1-15-1 Kitasato, Minami-ku, Sagamihara, Kanagawa 252-0373, Japan

ABSTRACT

The high intensity afforded by ultraviolet light is advantageous for laser-assisted scribing of advanced materials, including light-absorbing layers and electrode materials in solar cells. However, the wavelength conversion efficiency decreases in a nonlinear optical crystal at ultraviolet wavelengths due to the crystal's increased absorption of light at these wavelengths. We have devised a method to analyze wave equation by coupling them with a heat conduction equation in order to clarify the relationship between reduction in conversion efficiency due to phase mismatching and the temperature distribution inside the crystal. Fourth-harmonic-generation laser light was passed through a β-barium borate crystal to confirm the validity of the analysis method. This method allows a quantitative assessment of the effect of the relationship between light intensity and crystal length on wavelength conversion, and can be used to select the optimum crystal length.

Keywords: *wavelength conversion, BBO crystal, heat influence analysis, SHG, FHG*

1. INTRODUCTION

Solid-state lasers recently have been used for patterning electronic circuits of solar cell panels, laser patterning devices equipped with solid-state lasers have been produced. However, to improve power generation efficiency in solar cells, miniaturized circuitry is required, which in turn requires lasers with emission wavelengths shorter than those of our solid-state lasers. The higher intensity afforded by ultraviolet (UV) light also has become more necessary for scribing advanced materials such as electrodes and light-absorbing layers.

In patterning processes, several nonlinear optical crystals are commonly used in conjunction with solid-state lasers whose wavelength is almost 1 μm, thus enabling second harmonic generation (SHG) and fourth harmonic generation (FHG). FHG is particularly important for various applications of UV laser light, nonlinear optical crystals such as CLBO, LBO, β-barium borate (BBO) and KDP are widely used for FHG. However, decreasing laser wavelength and increasing laser intensity result in increasing light absorption, causing some heat problems where wavelength conversion efficiency might be attenuated by temperature distribution in the crystal.

To devise an efficient temperature control method and thus more effectively utilize the laser light, these heat problems must be elucidated. Toward this goal, several studies have been published. For example, Eimerl computationally analyzed the effect of increasing temperature on wavelength conversion efficiency in BBO crystals [1]. Kang's group worked on optimizing wavelength conversion by adjusting the BBO crystal length to stabilize SHG [2], and the effects of laser intensity and crystal length on wavelength conversion efficiency were analyzed in detail by Li using KDP crystals [3]. However, the influence of the relationship between laser intensity and crystal length on wavelength conversion efficiency has not been systematically studied. Therefore, in this study, we investigated wavelength conversion efficiency in a BBO crystal by means of numerical simulation expressed in both wave equation and a heat conduction equation. We selected BBO owing to its higher UV light transmittance, nonlinear coefficient, and damage threshold compared with the other crystals. To verify the numerical simulations, we compared our calculated results with experimental results, in which FHG was generated from SHG of a Nd:YAG laser.

2. BASIC EQUATION AND CALCULATION METHOD

2.1. LIGHT PROPAGATION EQUATION

In this section, we analyze wave equation for propagation of an electromagnetic wave in a crystal. An equation expressing light propagation in a crystal can be written as follows:

$$\frac{\partial^2}{\partial x^2} E_1 - \varepsilon\mu_0 \frac{\partial^2}{\partial t^2} E_1 = 0 \ , \qquad (1)$$

where E_1 is the electric field generated by a laser, x is the distance along the light axis, t is time, ε is permittivity, and μ_0 is space permeability. Nonlinear polarization P is caused by nonlinear effects when the laser propagates inside the crystal. The propagation equation including nonlinear polarization can be expressed as

$$\frac{\partial^2}{\partial x^2} E_2 - \varepsilon\mu_0 \frac{\partial^2}{\partial t^2} E_2 = \mu_0 \frac{\partial^2}{\partial t^2} P \, , \qquad (2)$$

where E_2 is the electric field caused by P. Equations related to the complex amplitude of the electric field are additionally obtained from equations (1) and (2). The growth process of the FHG component generated in the crystal can be analyzed by solving the complex amplitude equations.

2.2. HEAT CONDUCTION EQUATION

Heat is produced in the crystal due to the absorption of light. Heat conduction in the crystal is expressed as

$$\rho c \frac{\partial T}{\partial t} = k \frac{\partial^2 T}{\partial x^2} + k \frac{\partial^2 T}{\partial y^2} + w, \qquad (3)$$

where w [W/m^3] is the calorific power per unit time and volume, ρ is the crystal density, c is the calorific capacity, T is temperature, k is the crystal thermal conductivity, x is the distance along the light axis, y is the distance perpendicular to the light axis, and t is time. As shown here, since the heat conduction equation is two dimensional, the temperature distribution is also two dimensional. In contrast, the wave equation is one dimensional. A typical value of temperature is required to calculate the wave equation. The quantity w is estimated from the attenuation of light intensity by self-reduction as

$$w = -\frac{dI}{dx} \, , \qquad (4)$$

where I is the light intensity in the crystal.

2.3. PHYSICAL PROPERTIES OF THE BBO CRYSTAL

The BBO crystal's optical and thermal properties, such as refractive index, thermal conductivity, and absorption coefficient, are necessary to analyze its wavelength conversion efficiency. The physical properties of the BBO crystal used in the present simulation are shown in Tables 1 through 3. Table 1 is physical properties containing nonlinear coefficient which is most basic for analysis [4]. Although these numerical values are obtained from several literature sources [1] [4], the absorption coefficient was quoted from nonlinear optics crystal software (SNLO) [5], which was developed by Sandia National Laboratories. The distribution of transmittance as a function of wavelength can be obtained from SNLO, but the value is eliminated the effect of surface reflection caused by refractive index. Hence, the absorption coefficient can be obtained from the transmittance immediately. To compare the calculated results with experimental results using actual crystals, reflectance losses, such as those owing to deliquescent resistance coating on the crystal, must be taken into consideration.

Table 2 lists the Sellmier coefficients for the crystal, reported for both ordinary (n_o) and extraordinary (n_e) refractive indices [1]. The numerical values in Table 2 represent the constants in the following equation:

$$n^2 = A + \frac{B}{\lambda^2 + C} + D\lambda^2 \, , \qquad (5)$$

Temperature differentiations of the refractive index, which are necessary for the simulation, are shown in Table 3 [1]. Refractive index is a function of temperature and is expressed as

$$n(T) = n_{T=T_0} + \frac{\mathrm{d}n}{\mathrm{d}T} \Delta T \, , \qquad (6)$$

where ΔT is the variation from the temperature $T=T_0$.

Table 1. Optical and thermal properties of BBO crystals.

Nonlinear coefficient	2.00×10^{-23} [Fm^{-1}]
Density	3840 [kg m^{-3}]
Specific heat at 293K	490 [J kg^{-1} K^{-1}]
Thermal conductivity at 293K	1.60 [W m^{-1} K^{-1}]
Absorption coefficient for 532-nm	0.269 [m^{-1}]
Absorption coefficient for 266-nm	10.26 [m^{-1}]

Table 2. Sellmeier coefficient of BBO crystals.

	A	B	C	D
		μm^2	μm^{-2}	μm^{-2}
n_e	2.3730	0.0128	-0.0156	-0.0044
n_o	2.7405	0.0184	-0.0179	-0.0155

Table 3. Temperature dependence of refractive index of BBO crystals.

λ [μm]	$dn_e/dT\times10^6$ [K^{-1}]	$dn_o/dT\times10^6$ [K^{-1}]
1.0410	-9.76	-16.64
0.5790	-9.42	-16.35
0.4047	-8.84	-16.83

2.4. CALCULATION MODEL AND METHOD

As mentioned previously, heat is produced in the crystal due to the absorption of laser light. The absorption varies, as evidenced by shifts in the phase matching angle, when the refractive index is influenced by temperature variation. However, heat is also liberated from the crystal surface, and it takes certain time to become an equilibrated state where heat is stationary liberated in the calculation. In other words, a stationary solution cannot be obtained by the analysis of a single laser pulse. To obtain the stationary solution, the laser pulse is repeated until the crystal temperature equilibrates.

Evaluating complex amplitudes by solving simultaneous differential equations of incident light and converted light is necessary to calculate the attenuation of incident light and the growth of converted light. We then calculated the total amount of light intensity in the crystal using the following equation:

$$I = \frac{\varepsilon_0 c E^2}{2}, \qquad (7)$$

The I value obtained from this equation was then used in equation (4) to calculate calorific power. Finally, a stationary solution was obtained by calculating the temperature distribution based on equation (3).

We calculated the wavelength conversion efficiency, including heat produced due to light absorption. The calculation is a cylindrically shaped crystal as shown in figure 1. The central axis of the crystal equals the optical axis used in the calculations, and the region of laser irradiation is illustrated by diagonal lines in figure 1. The calculation conditions and the flow chart used in the simulation are shown in Table 4 and figure 2, respectively.

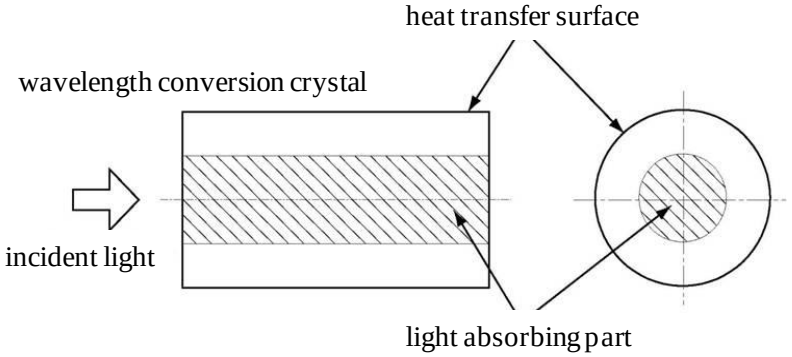

Figure. 1. Calculation model.

Table 4. Simulation condition.

β-BBO crystal		
radius		6.0 mm (mesh size:0.3mm/mesh number:20)
length		2.0, 4.0, 6.0 mm (mesh size:0.3mm/mesh number:20)
heat transfer coefficient	side	100.0 $W/m^2 K$
	surface	10000.0 $W/m^2 K$
laser		
pulse width		10 ns
repetition frequency		10 Hz
beam radius		3.0 mm
power density		2.0×10^{11}, 4.0×10^{11}, 6.0×10^{11}, 8.0×10^{11}, 1.0×10^{12} W/m^2
average output power		0.566, 1.13, 1.70, 2.26, 2.83 W
calculation parameter		
time step		10 ns
initial temperature	crystal	293 K
	surrounding air	293 K

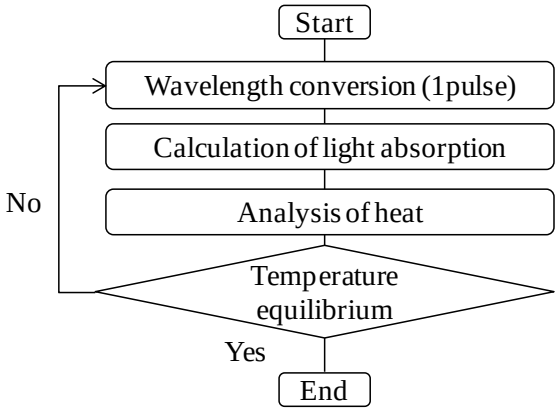

Figure 2. Calculation flow chart

The calculation process can be described as follows: Wavelength conversion in a single pulse of laser irradiation is first analyzed to estimate the light absorption in the crystal. Then, the heat generated due to the light absorption is analyzed during the pulse interval. This process is repeated many times until the crystal temperature reaches an equilibrium value, which we considered to be the stationary solution.

3. CALCULATION RESULTS

3.1. ARRIVAL TIME OF TEMPERATURE EQUILIBRIUM

As shown in figure 2, the calculation process was repeated until the crystal temperature reached equilibrium. Figure 3 shows the variations of crystal temperature for crystal lengths l = 4.0 and 6.0 mm at a laser intensity of 1.0×10^{12} W/m^2. The temperature variation was calculated at the center of the crystal, and it was confirmed that the temperature equilibrium actually was reached. The temperature variation for every pulse is plotted in figure 3 simultaneously, and a temperature variation threshold value was established to determine whether equilibrium had been reached. For l = 4.0 and 6.0 mm, temperature equilibrium was reached after 92 and 168 pulses, respectively, for an equilibrium threshold value of 1.0×10^{-4} K/pulse. Therefore, 100 and 200 pulses, respectively, were considered to be sufficient for obtaining a stationary solution. In the following calculation, we define 200 pulses as the number of pulses after which temperature equilibrium is established.

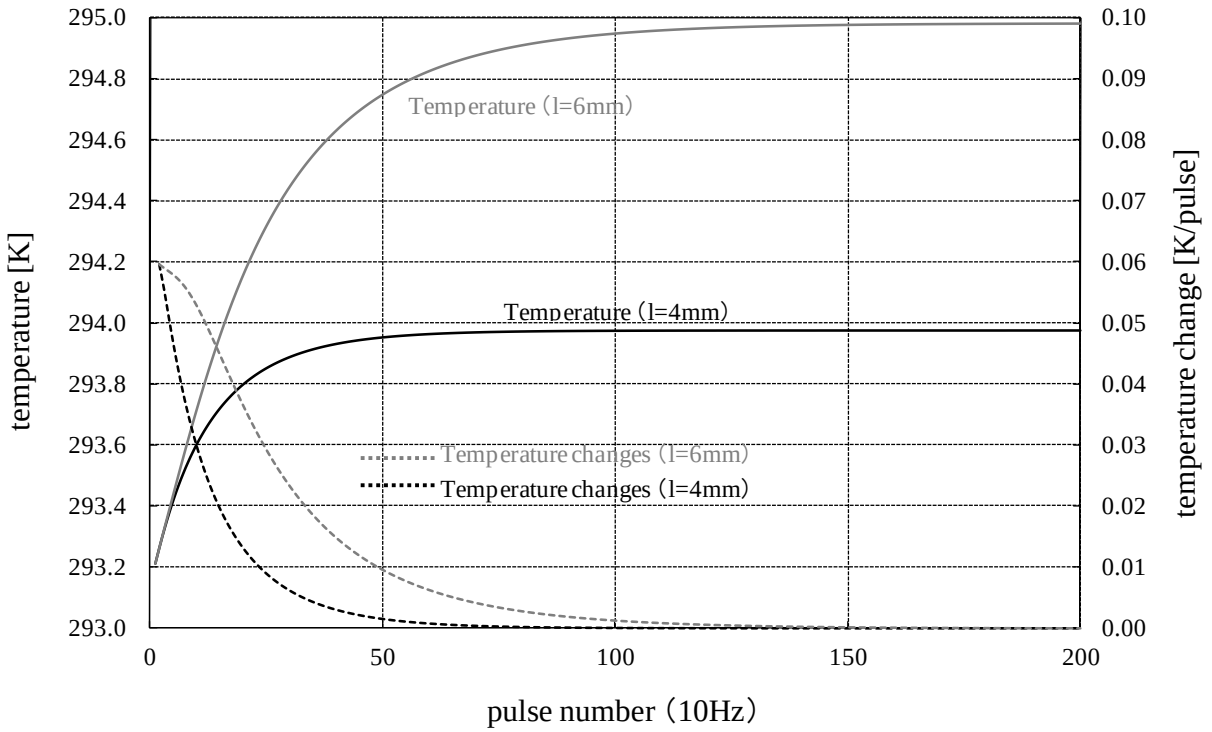

Figure 3. Calculation result of temperature equilibrium.

3.2. LASER INTENSITY DISTRIBUTION AND WAVELENGTH CONVERSION EFFICIENCY IN THE CRYSTAL

We calculated the FHG wavelength conversion efficiency and temperature distribution for various crystal lengths. Figure 4 shows the intensities of SHG (incident light) and FHG (converted light) and the temperature distribution for crystal length l = 6.0 mm.

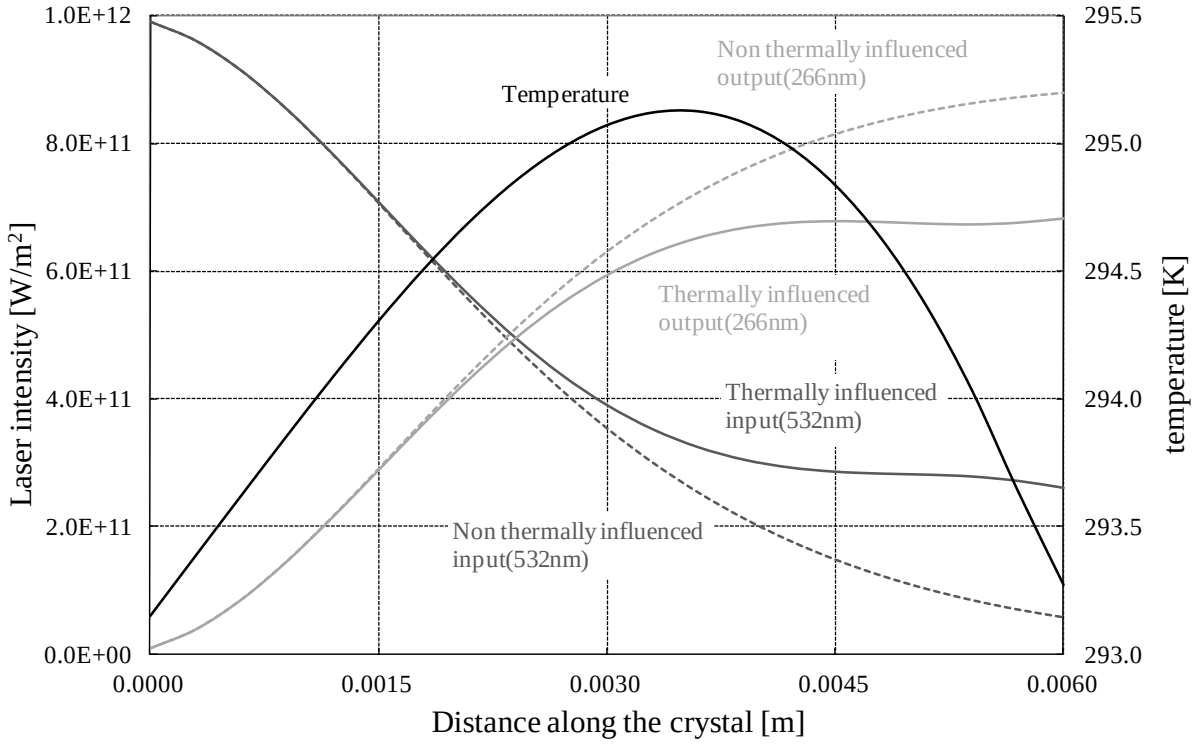

Figure 4. Calculation results of frequency conversion and temperature distribution (l =6.0mm).

The left side of the graph corresponds to the incident plane of the SHG light, which possesses an intensity of 100%. It was confirmed that the incident light is attenuated with generating FHG as it proceeds into the crystal. The temperature distribution along the central axis at equilibrium is also plotted in figure 4. The maximum temperature appeared at the distance of x = 3.5 mm, which is located at slight backside along the crystal axis. This observation suggests that the calorific power of absorption increased with generating FHG at the backside location. The liberation of heat at the crystal surface depressed the temperature at the left and right sides of the graph. Additionally, both thermally and non-thermally influenced laser intensities in the crystal are plotted in figure 4. The thermally influenced laser intensity (solid line) began to deviate from the non-thermally induced laser intensity (dashed line) at x = 2.0 mm for both SHG and FHG, and the conversion efficiency declined significantly for the thermally influenced intensity. The maximum temperature increase was about 2.0 K. These results confirm that conversion efficiency was influenced by temperature. For l = 4.0 mm, the maximum temperature increase was about 0.85 K, which influenced the conversion efficiency less than 0.1%. In general, decreases in conversion efficiency are caused by the walk-off angle, thermal lens effect, nonlinear variation of refractive index, or shifts in phase matching angle due to light absorption. However, as discussed below, variation of refractive index due to changes in temperature owing to light absorption decreases the conversion efficiency more dramatically than these other factors.

The wavelength conversion efficiency was influenced by the intensity of the incident laser and by the length of the crystal. In figure 5, the wavelength conversion efficiency was calculated against the intensity of the incident laser at three crystal lengths. As is clearly shown in the figure, the conversion efficiency increases at longer crystal lengths and higher laser intensities. However, the conversion efficiency decreases if the laser intensity is too high, as in the case of the crystal length of 6.0 mm. That is, the optimum crystal length can be determined by considering the trade-off between the advantage of crystal length and the disadvantage of heat influences.

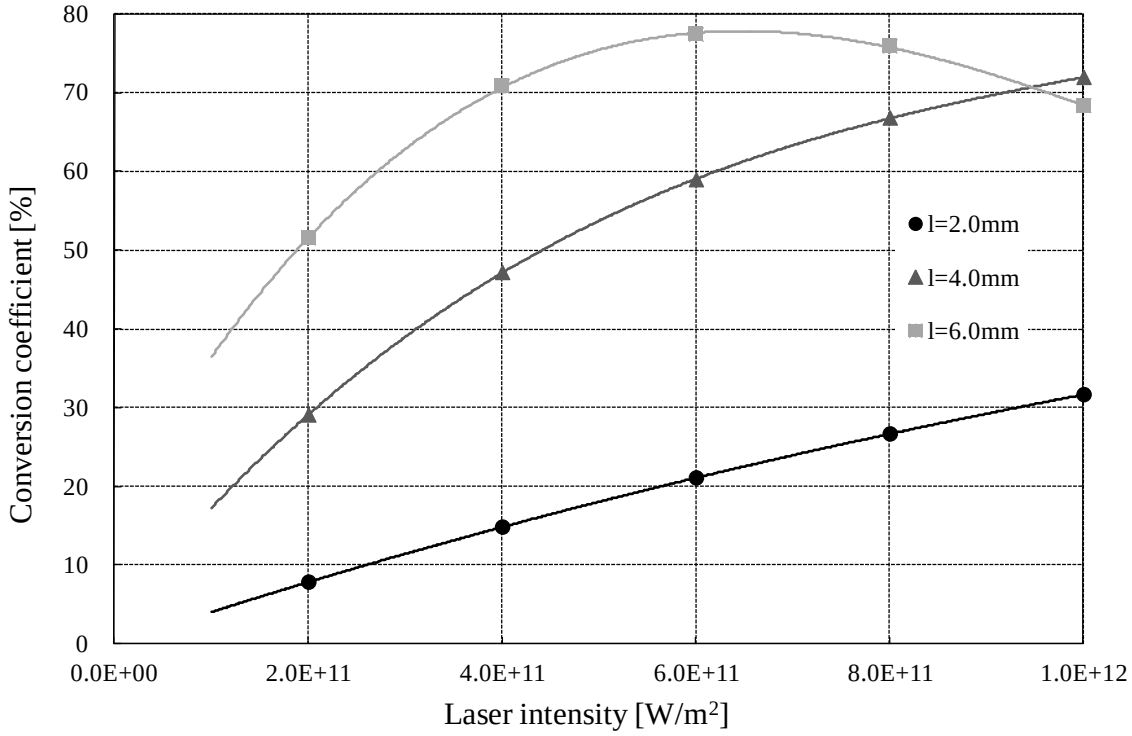

Figure 5. The influence of laser intensity for frequency conversion efficiency (calculation results).

4. DISCUSSION

4.1. THE INFLUENCE OF PHASE MISMATCHING

First, we discuss the loss of wavelength conversion efficiency due to phase mismatching. The condition of phase matching between the incident and the converted light is satisfied by means of birefringence phase matching. The dependence of the incident angle on the crystal refractive index is more obvious for an extraordinary beam than for an ordinary beam. Hence, the refractive index can be matched by adjusting the incident angle after adjusting the polarization, as incident light conforms to ordinary light and converted light conforms to extraordinary light. The relationship between the refractive index and the incident angle is given by

$$\frac{1}{n_e^2(\theta_i)} = \frac{\cos^2\theta_i}{n_o^2} + \frac{\sin^2\theta_i}{n_e^2}, \quad (8)$$

where θ_i is the incident angle. The difference between the wavenumber of incident light k_1 and that of converted light k_2 is expressed as

$$\Delta k = k_2 - 2k_1, \quad (9)$$

The inclination between the optical axis and crystal axis can be set to zero.

Figure 6 shows wavelength conversion efficiency influenced by phase matching wavenumber for crystal length l=6.0 mm. If we assume that FWHM of wavenumber is stable conversion, the allowable width of phase matching angle can be evaluated as 179 μrad.

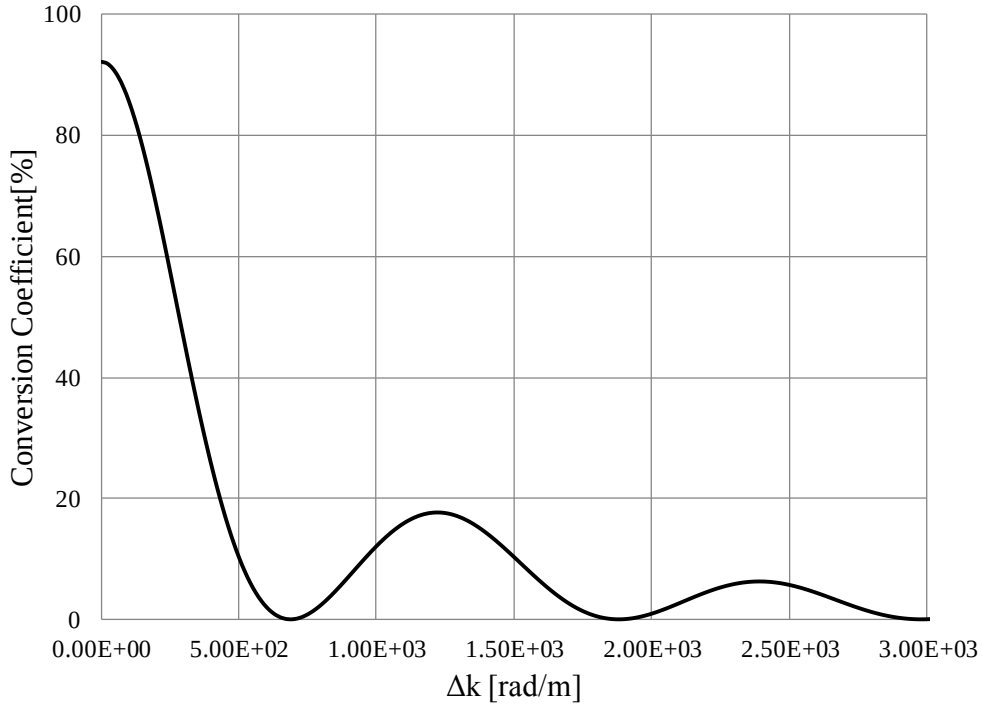

Figure 6. Wavelength conversion efficiency influenced by phase matching wavenumber

4.2. THE INFLUENCE OF THE THERMAL LENS EFFECT

Since a flat-topped form was assumed as the space distribution of laser, the temperature along the optical axis in the crystal was used as a typical value in the previous paragraph. However, the temperature distribution induced from the flat-topped form of laser beam inside the crystal is not complete flat-topped form due to the thermal diffusion. Figure 7 shows the temperature distribution in the central part of the crystal for a laser intensity of 1.0×10^{12} W/m^2 and crystal length of 6.0 mm.

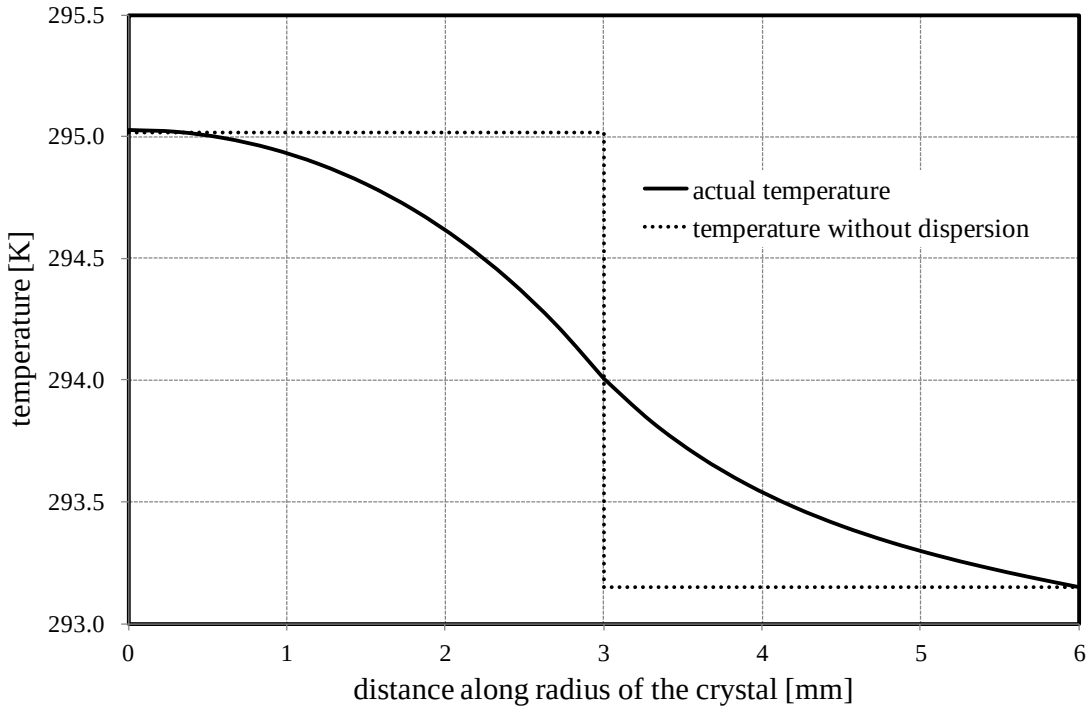

Figure 7. Temperature distribution at crystal central part.

The thermal lens effect is of practical importance since it induces a temperature distribution, which causes the phase mismatching. In this section, we examine the influence of the thermal lens effect on wavelength conversion efficiency. Figure 8 shows the refractive index distribution derived from the results of figure 7.

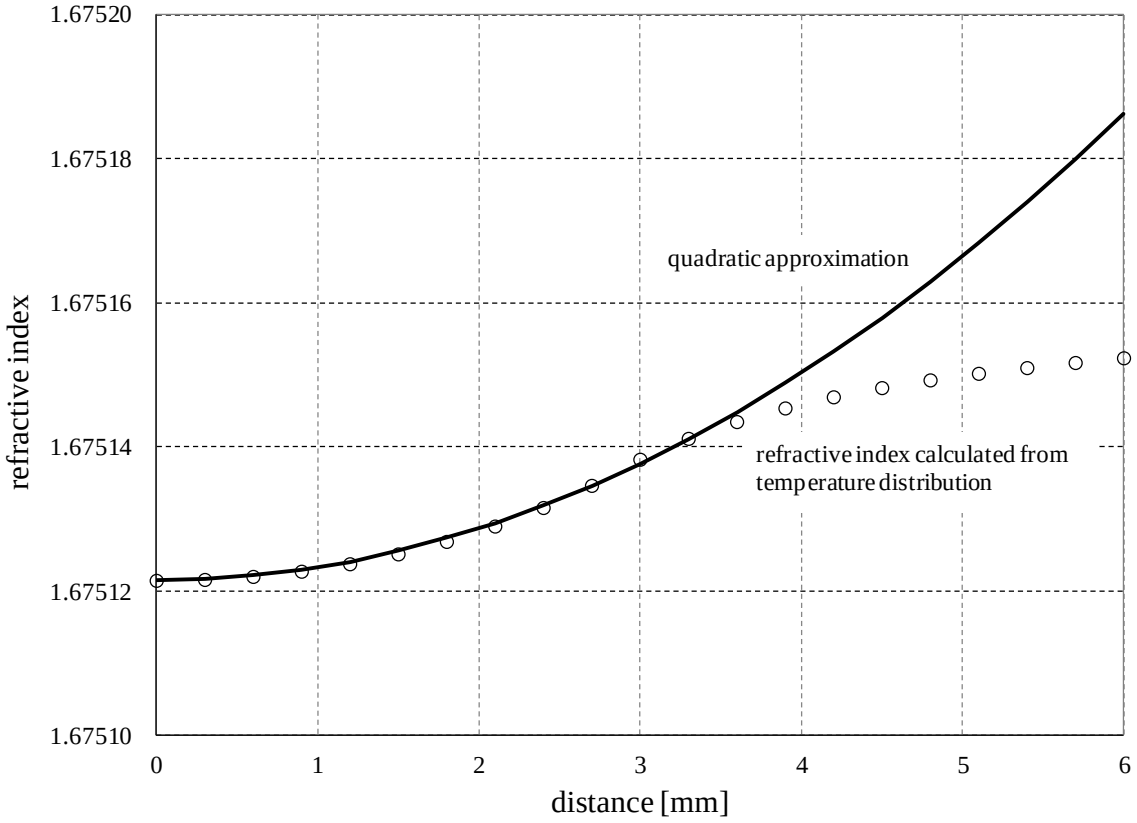

Figure 8. Refractive index distribution at crystal central part.

As listed in Table 3, the refractive index of the BBO crystal decreases at the temperature increases. Therefore, the refractive index in the central location is smaller than that in the peripheral domain. As a result, the laser beam tends to diffuse in the crystal due to the refractive index distribution, which is generally written as

$$n(r) = n_{r=0}\left(1+\frac{2r^2}{b^2}\right), \qquad (10)$$

where r is the radius of a cylindrically shaped crystal, $n_{r=0}$ is a refractive index of center of crystal axis and b is a constant number which derived from quadratic approximation of figure 8 [6]. Then, the deflection angle θ_t caused by the thermal lens effect is calculated as

$$\theta_t = \tan^{-1}\left(\frac{R}{f}\right), \qquad (11)$$

where R is the radius of the laser beam and f is the focus length caused by the thermal lens effect, expressed as

$$f = \frac{b^2}{4n_{r=0}L}, \qquad (12)$$

where it is estimated that b is 1364 mm and θ_t is 65 μrad by using equation (10) and (11).

4.3. THE INFLUENCE OF THE WALK-OFF ANGLE

The pointing vector of the extraordinary beam has a certain deflection angle relative to the incident laser beam direction due to crystal birefringence. If the laser beam diameter is small, then the converted beam generated in the crystal diverges from the incident beam by a walk-off angle, causing degradation of the conversion efficiency. The effective crystal length is expressed as

$$L_{eff} = \frac{r}{\tan\rho}, \qquad (13)$$

where L_{eff} is effective crystal length, ρ is walk-off angle. For the BBO crystal, the phase matching angles was 85.30 mrad against wavelength of 532 nm [5]. The effective distance for the conversion is about 35mm for our simulation condition, which is larger than our crystal length.

4.4. THE INFLUENCE OF PULSE FORM

The wavelength conversion efficiency is also influenced by the time variation of the laser pulse. Although the pulse form of the laser beam was assumed to be a rectangular wave in our calculations, the wavelength conversion efficiency can be expected to depend on variations in the pulse form. For example, for a Gaussian distribution of laser intensity, the conversion efficiency at the edges of the distribution, where the intensity is weakest, decreases because the low-intensity light is not able to contribute to wavelength conversion. Therefore, it is necessary to calculate the conversion efficiency per pulse by measuring the intensity of the converted light in small time intervals and temporally averaging those values. In addition, the laser pulse that was used in the experiment was measured with a photodiode and employed as an incident laser beam in the simulation. The measured pulse form is shown in figure 9.

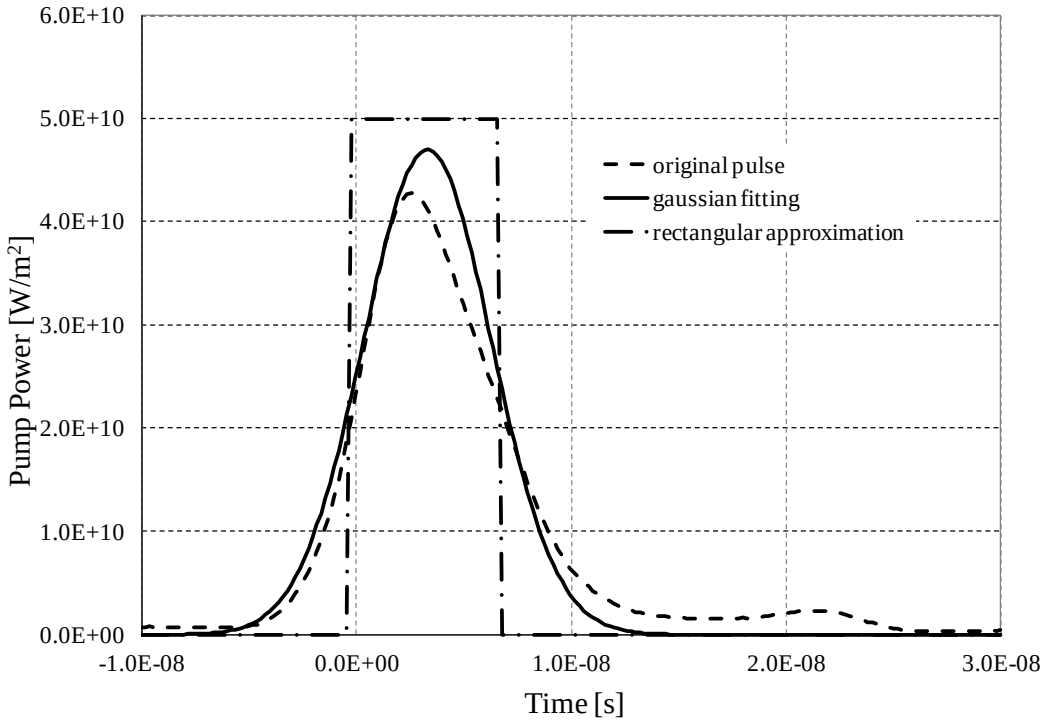

Figure 9. Approximation model of laser pulse.

While the actual pulse form is represented as a solid line in figure 9, the pulse form was approximated by a Gaussian distribution (dashed line) as a matter of convenience of calculation. For reference, a pulse form approximated by a rectangle wave is also shown in figure 9. These waveforms are all normalized so that the laser energy per pulse of every form is the same.

The calculated results of wavelength conversion efficiency for both the rectangular wave and the Gaussian approximation are shown in figure 10.

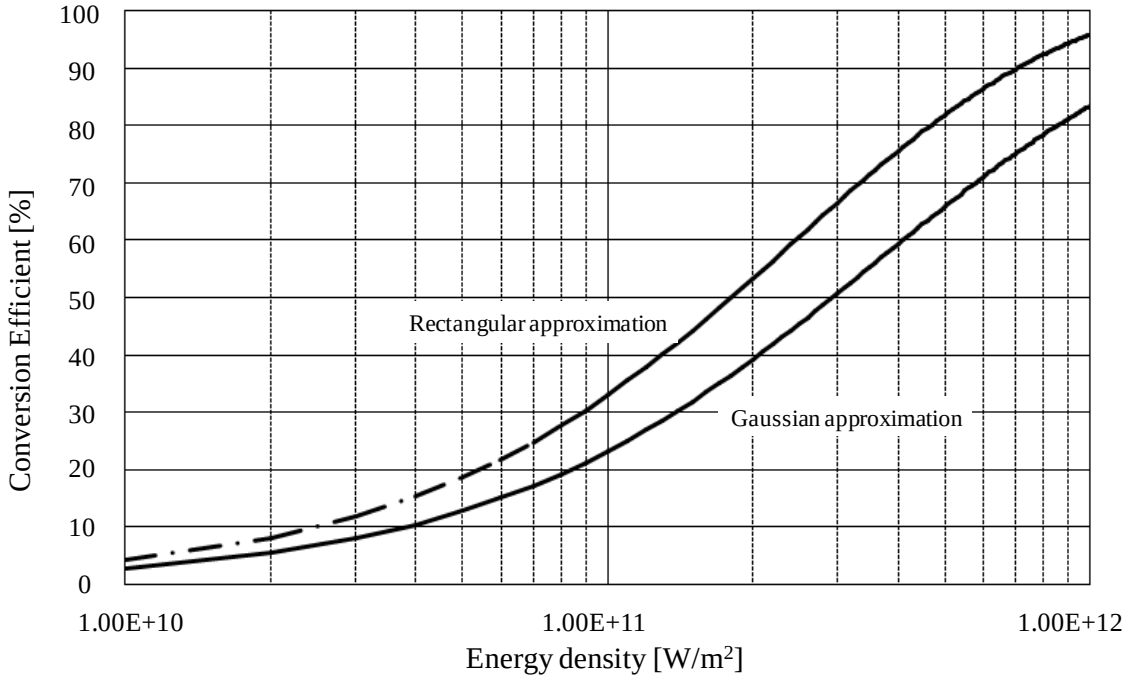

Figure 10. The influence of approximation model of laser pulse against wavelength conversion efficiency.

Although every conversion efficiency monotonically increases with increasing incident light intensity, the inclination for the rectangular approximation is sharper. Actually, it could be expected that the closer the pulse form is to the rectangular, the higher the conversion efficiency is. The conversion efficiency for the pulse form approximated by the Gaussian was about 10% lower than that by the rectangular wave as shown in figure 10.

4.5. COMPARISON WITH EXPERIMENTAL RESULTS

The following experiments were carried out to demonstrate the validity of the wavelength conversion calculations. Light emitted from a laser oscillator impinged upon a BBO crystal as a test sample after adjusting output power through a wavelength plate and a polarizing beam splitter (PBS). Only the converted light passing through the crystal was introduced to a power meter by a dichroic mirror. The power was measured after the power meter stabilized; date were acquired for 10 minutes and then statistically treated. The wavelength conversion efficiencies were calculated with consideration of optical losses owing to optics inserted in the system, the losses from which had been measured in advance. The resulting wavelength conversion efficiencies are plotted against incident laser intensity in figure 11. In this figure, the conversion efficiencies, which are plotted for various crystal lengths, are all about 30% at maximum. The optimum crystal length depends on the incident intensity, with shorter crystals generally requiring higher laser intensities to yield high conversion efficiency. This is because the change of refractive index can be caused by increasing the inclination of temperature for the reason remarked in the previous paragraph, although the effective distance for the conversion is earned in the longer crystal. Thus, compared to the results shown in figure 5, these experimental results coincided closely with the calculations obtained for the shortest crystal (l = 2.0 mm). However, for the longest crystal (l = 6.0 mm), no exact coincidence between experiment and calculation was apparent, since it is difficult to actually estimate the thermal boundary conditions of the crystal surface. Thus it will be necessary to verify the validity of thermal analysis by precisely measuring the crystal temperature and the absorption coefficient of the laser in future studies.

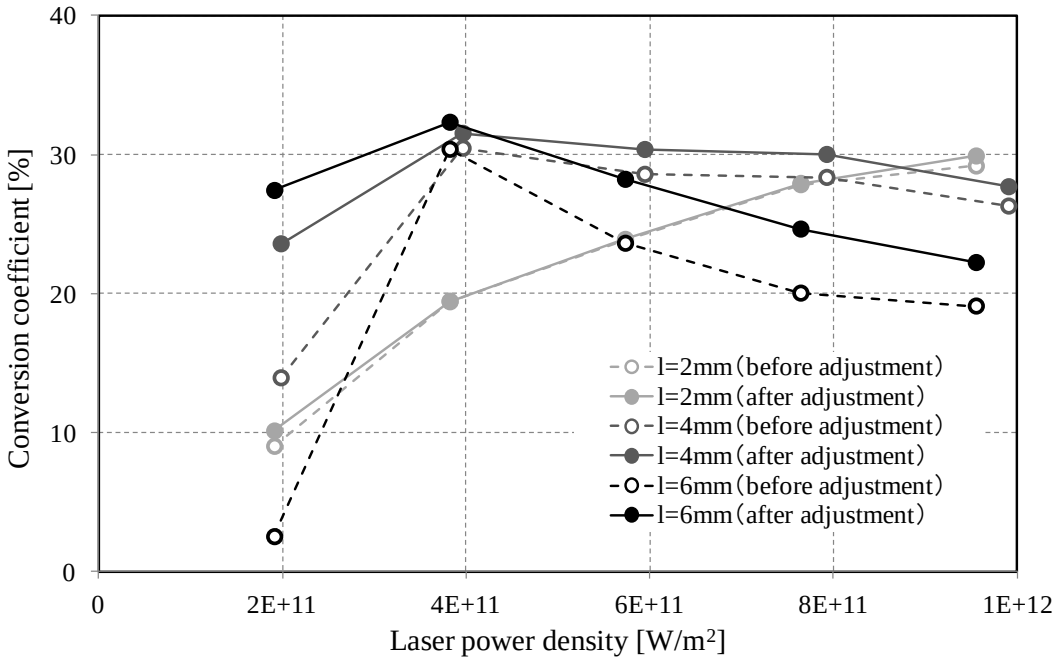

Figure 11. The influence of laser intensity against frequency conversion efficiency (experiment results).

5. CONCLUSIONS

To enable the design of wavelength conversion devices utilizing BBO nonlinear optical crystals, the relationship between the temperature distribution in the crystal and the degradation of wavelength conversion efficiency due to phase mismatching was quantitatively studied by simulation. We found that the temperature distribution in the crystal was related to the absorption of incident laser light, as well as to the distribution of FHG and SHG. Hence, the necessity of positive cooling of the crystal can be suggested, in order to adjust the phase mismatching angle resulting from thermal effects. Our results confirm that BBO crystals can be used efficiently for wavelength conversion if the length of the crystal and the intensity of the laser are optimally selected by conducting the thermal simulation.

Our results also confirm that thermal equilibrium was reached, so the numerical solution to the simulation converged to include self-absorption of the laser. Furthermore, an appropriate crystal length for efficient wavelength conversion could be selected by quantitatively reviewing the dependence of crystal length on the wavelength conversion efficiency. These calculated results were compared with experimental results, and the validity of the present simulation was confirmed by considering the temperature distribution, the approximation of the laser pulse, the thermal lens effect, and the walk-off angle.

Finally, the simulation used in the present study enables the prediction of variations in wavelength conversion efficiency among different types of crystals by accounting for factors such as the nonlinear coefficient, absorption coefficient, refractive index, and thermal conductivity. In future studies, we plan to apply this simulation to a continuous oscillation laser, to develop a database of nonlinear optical crystal information, and to predict optimum materials for wavelength conversion.

6. REFERENCES

[1] H. J. Eimerl et al., "Optical, mechanical, and thermal properties of barium borate", J. Appl. Phys. 62-5, 1987, 1968-1983

[2] J. Kang et al., "Design of a highly stable, high-conversion-efficiency pumping source for optical parametric amplifier by extending efficient crystal length" Optics & Laser Technology 39, 2007, 1084–1088

[3] K. Li et al., "Theory and experiment analysis of factors affecting THG efficiency for the TIL prototype laser facility" Optik 120, 2009, 1–8

[4] N. P. Barnes et al., "Average power effects in parametric oscillators and amplifiers" J. Opt. Soc. Am. 12, 1995, 124–131

[5] SNLO nonlinear optics code available from A. V. Smith, Sandia National Laboratories, Albuquerque, NM 87185-1432.

[6] W. Koechner, "Solid-State Laser Engineering" Berlin: Springer, 1999